Response to Reviewer 1 Comments

1. Summary

Thank you for overseeing the review process of our manuscript. We are pleased to submit the revised version of our manuscript, titled *"A Label-Free Colorimetric Aptasensor for Flavokavain B Detection."* We greatly appreciate the insightful and constructive comments provided, which have helped us improve our study.

In this revised manuscript, we have addressed all the suggestions, with changes highlighted in red text and our detailed responses included in blue text.

2. Point-by-point response to Comments and Suggestions for Authors

Comments 1: *Why chose the absorbance ratio (A650/A520) as the y-axis to develop the standard curve? Why not use the absorbance at A650 or A520?*

Response 1: Thank you for the reviewer's question. In the gold nanoparticle-based colorimetric assay, using the absorbance ratio at two wavelengths to determine the linear range is a widely adopted strategy (**Nature Protocols, 2006, 1(1): 246-252; Microchimica Acta, 2018, 185: 1-6; Sensors and Actuators B: Chemical, 2023, 390: 133968**). The primary purpose of this approach is to enhance the sensitivity and anti-interference capability of the detection.

The specific reasons are as follows:

1. The change in absorbance at a single wavelength is relatively small, making it difficult to detect subtle signal variations. In contrast, using the absorbance ratio can significantly amplify these minor signal changes, enabling more sensitive and accurate detection of low-concentration samples.
2. The absorbance at a single wavelength is more susceptible to experimental condition fluctuations (e.g., solvent background, nonspecific absorption in the sample), leading to signal instability. By calculating the ratio of absorbance at two wavelengths, these interference factors can be effectively minimized.

Comments 2: *The ruler is missing in Figure 4 b-c.*

Response 2: We apologize for the previous ruler being unclear, which may have caused confusion. We have revised and clearly labeled the ruler in the **Figure 4 b-c**.

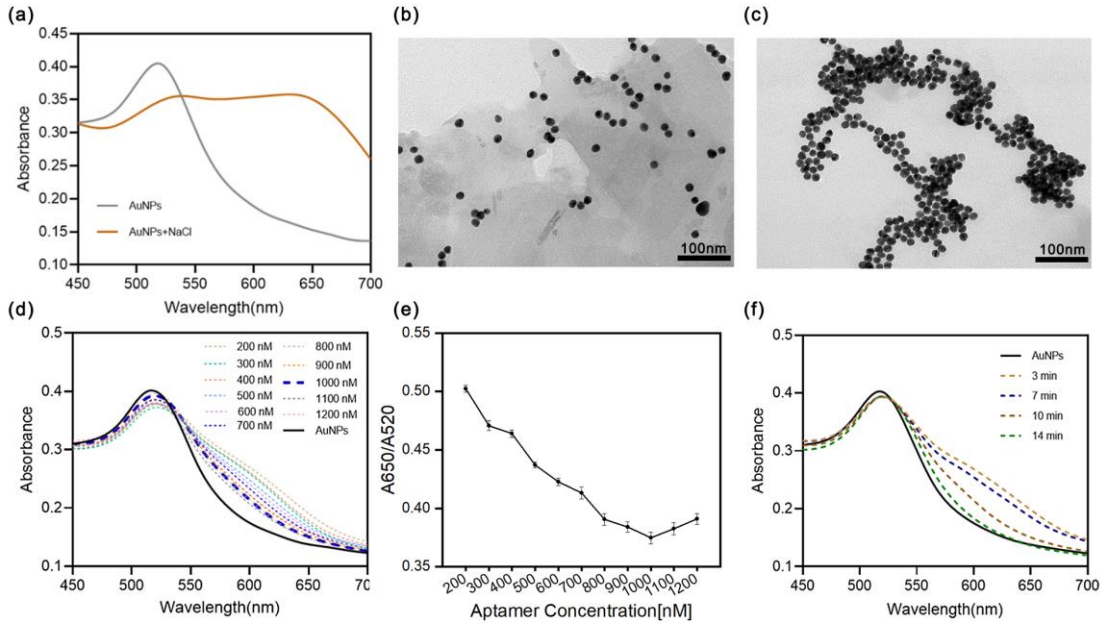


Figure 4. (a) UV/Vis spectra of AuNPs and aggregated AuNPs induced by NaCl. TEM image of (b) AuNPs and (c) aggregated AuNPs. (d) UV/Vis spectra of AuNPs at varying FKB-S concentrations, with (e) the corresponding absorbance ratio (A650/A520). (f) Time-dependent UV/Vis spectral changes of AuNPs during incubation with 1 μM FKB-S.

Comments 3: *In Figure S2, it seems that the ratio of A650/A520 was increased with the NaCl concentration from 150 to 400 mM. Why not study the higher NaCl concentration than 400 mM? Is it reasonable that of 400 mM as the optimal NaCl concentration?*

Response 3: Thank you for your thoughtful question. We carefully considered the selection of NaCl concentration during the experiments. NaCl plays a crucial role in this process: it not only induces the aggregation and color change of gold nanoparticles but also facilitates the formation of the appropriate secondary structure of the aptamer, enabling its binding functionality.

To optimize the binding performance of the aptamer, we aimed to maintain an environment as close as possible to the selection conditions, specifically 1× Buffer (containing 10 mM Tris-HCl, 0.5 mM $MgCl_2$, 20 mM NaCl, pH 7.4). Therefore, we adopted a conservative strategy when adding NaCl, aiming to achieve gold nanoparticle aggregation with the minimum amount of NaCl necessary.

As shown in **Figure S2a**, when 20 μL of 400 mM NaCl and 60 μL of 1× Buffer were added, the NaCl concentration in the system was approximately 51 mM. At this concentration, significant aggregation of the gold nanoparticles was observed, with a notable decrease in the absorption peak at 520 nm. This NaCl concentration and the corresponding UV-Vis spectrum are consistent with previous reports (**Food Chemistry, 2024: 139944**). Furthermore, the growth of the A650/A520 ratio slowed and reached a plateau (**Figure S2a**). Based on these observations, we ultimately selected the protocol involving the addition of 20 μL of 400 mM NaCl.

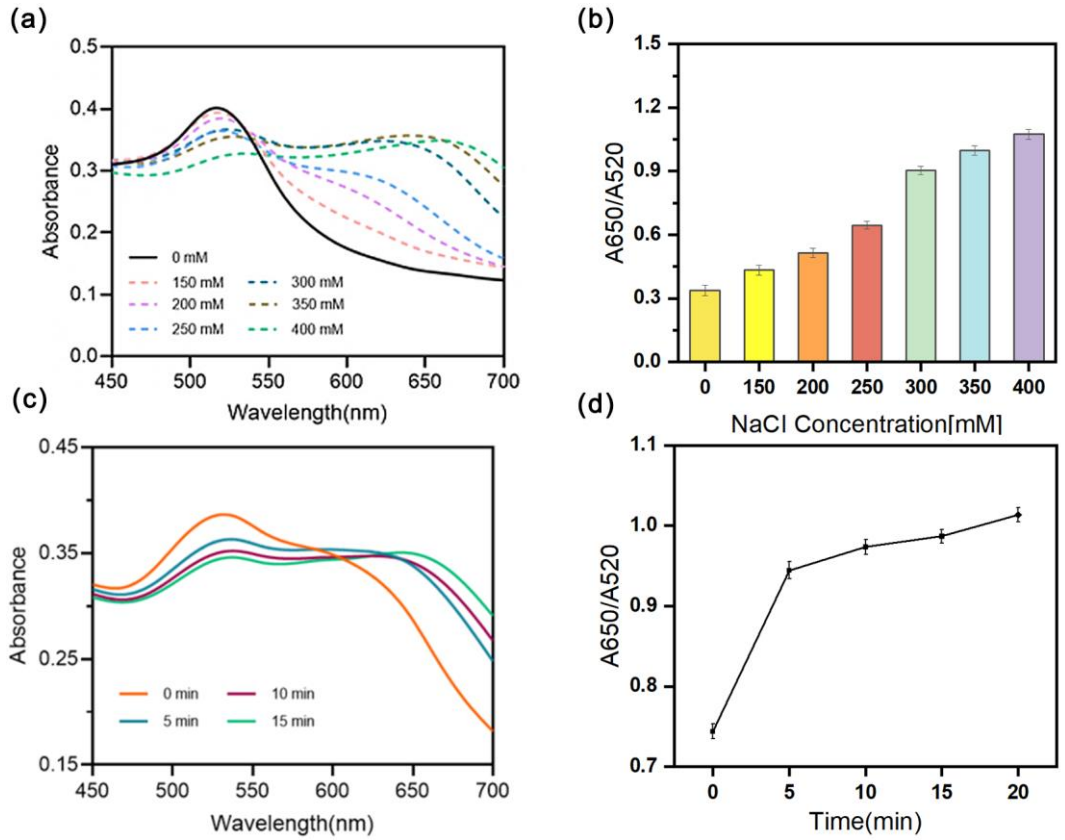


Figure S2. Optimization of NaCl concentration (a and b) and reaction time (c and d) in the aptasensor.

Comments 4: *The error bar is missing in some figures, such as Figure 4e, Figure S2 (b and d).*

Response 4: Thank you for your suggestion. These images have been revised and updated to include error bars.

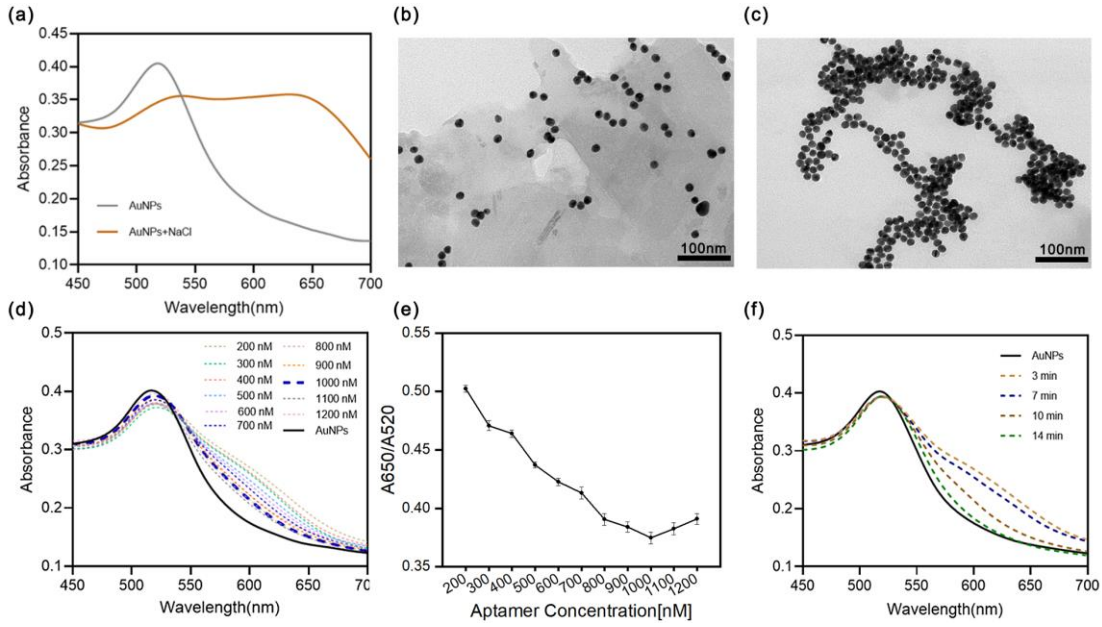


Figure 4. (a) UV/Vis spectra of AuNPs and aggregated AuNPs induced by NaCl. TEM image of (b) AuNPs and (c) aggregated AuNPs. (d) UV/Vis spectra of AuNPs at varying FKB-S concentrations, with (e) the corresponding absorbance ratio (A650/A520). (f) Time-dependent UV/Vis spectral changes of

AuNPs during incubation with 1 μM FKB-S.

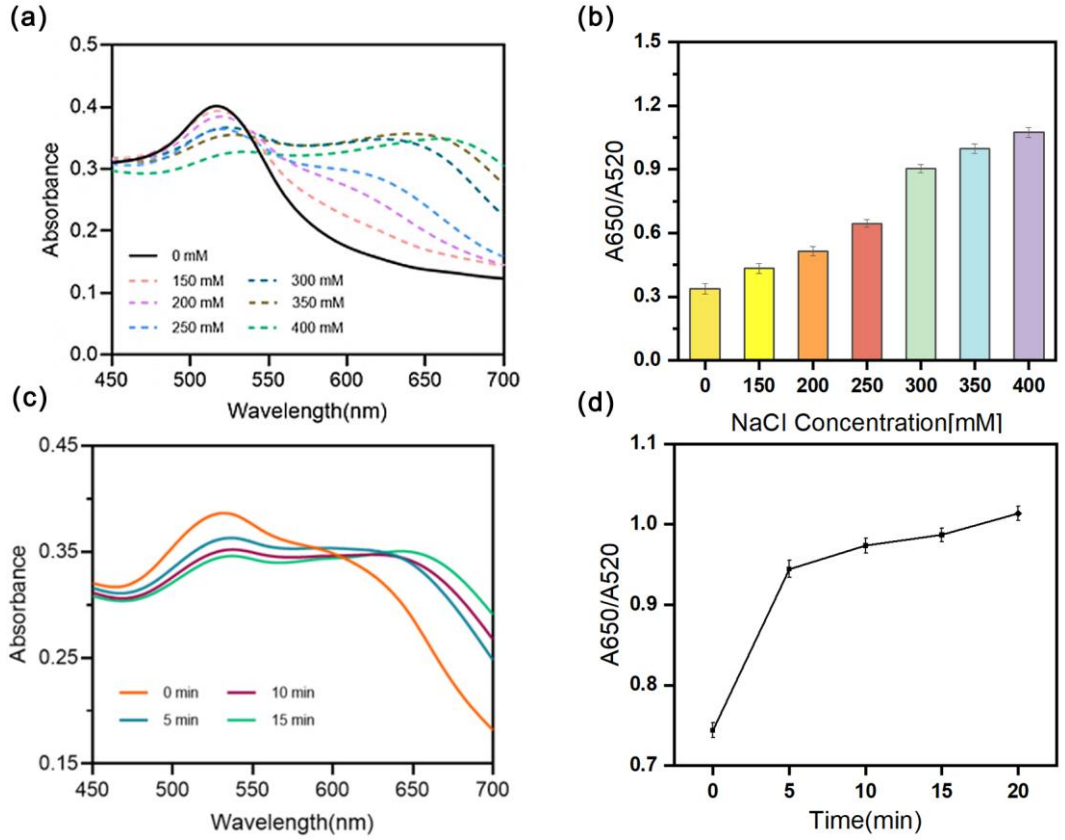


Figure S2. Optimization of NaCl concentration (a and b) and reaction time (c and d) in the aptasensor.

Comments 5: *In Figure 4e, how to get the conclusion that the binding reached equilibrium at 14 minutes. Because there lacks experiments with longer reaction time than 14 minutes for NaCl-AuNPs.*

Response 5: As shown in **Figure 4f**, after the addition of the aptamer, its protective effect on gold nanoparticles gradually became evident with increasing incubation time. Specifically, the absorption peak at 650 nm continued to decrease until, at 14 min, the absorption spectrum closely resembled that of gold nanoparticles without NaCl, with the absorbance at 650 nm returning to a level comparable to the original gold nanoparticle solution. Meanwhile, during the incubation period from 3 to 14 min, the absorbance at 520 nm remained stable without significant changes. Considering time efficiency, we concluded that an incubation time of 14 min is sufficient to meet the experimental requirements.

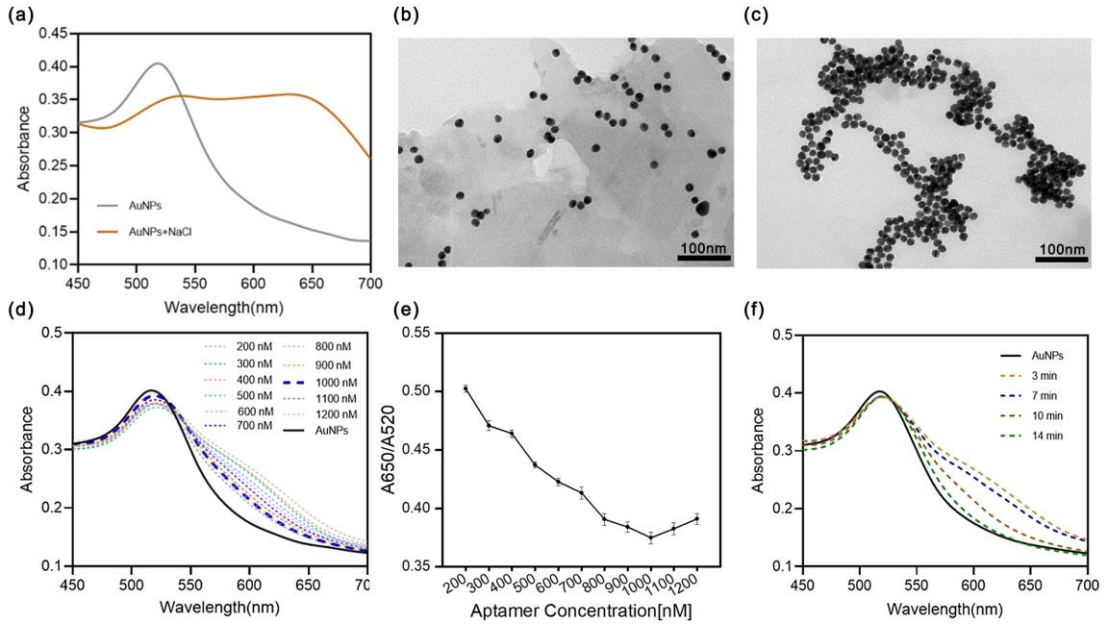


Figure 4. (a) UV/Vis spectra of AuNPs and aggregated AuNPs induced by NaCl. TEM image of (b) AuNPs and (c) aggregated AuNPs. (d) UV/Vis spectra of AuNPs at varying FKB-S concentrations, with (e) the corresponding absorbance ratio (A650/A520). (f) Time-dependent UV/Vis spectral changes of AuNPs during incubation with 1 μM FKB-S.

Comments 6: *Line 373-376, where is the relevant experimental results or figures in this part?*

Response 6: This section aims to clarify that a 5-minute incubation time was selected for evaluating the affinity between the aptamer and FKB, and this incubation time was consistently applied in subsequent detection method. The original manuscript lacked a detailed explanation of the microscale thermophoresis (MST) experimental procedure, which may have contributed to difficulties in reader comprehension. To address this issue, we have included a detailed description of the MST experimental steps in the revised manuscript and added appropriate references in the sections discussing the incubation time. These updates are intended to provide readers with a clearer and more accessible understanding.

2.6 Microscale Thermophoresis Assay

Affinity measurements were conducted using Microscale Thermophoresis on a Monolith NT.115 instrument. The aptamer, labeled at the 5′ end with a Cy5 dye (Table S1, FKB-1-5'FAM or FKB-S-5'FAM), was dissolved in MST buffer (10 mM Tris-HCl, 20 mM NaCl, 0.5 mM $MgCl_2$, 5% DMSO, 0.05% Tween-20, pH 7.4). The solution was heated at 95°C for 10 min and subsequently cooled on ice. FKB or potential interferents were prepared in MST buffer using a 2-fold serial dilution across 16 concentrations (10 μL per dilution). Next, 10 μL of the aptamer solution was mixed with 10 μL of each diluted sample and incubated for 5 min. The samples were then loaded into Monolith NT.115 standard capillaries. All experiments were performed independently in triplicate, and the data were analyzed using MO Affinity Analysis Software (Version 2.2.4).

Furthermore, the incubation time between the aptamer and its target has been extensively studied in similar research, with typical durations ranging from 5 to 10 min. This aligns with the 5-min incubation time used in the MST-based affinity characterization conducted in this study (Figure 3e). Accordingly, a 5-min incubation was adopted for FKB in subsequent experiments.

Comments 7: *In section 3.6, Figure 4 g-i is incorrect.*
Response 7: Thank you for your correction. The figure numbers have been revised in the manuscript and highlighted in red.

Under optimized experimental conditions, we evaluated the linear detection range and limit of detection of the aptasensor using varying concentrations of FKB. Figure 5a illustrates the changes in the UV/Vis absorption spectra observed when FKB, at concentrations ranging from 0 to 5 μM, was introduced into the Aptamer/AuNPs system. With increasing FKB concentration, the aptamer's protective effect on the AuNPs was progressively lost, resulting in nanoparticle aggregation and a corresponding increase in the A650/A520 ratio (Figure 5b). The corresponding linear relationship can be expressed as: $y=0.0817C+0.3941$ within the concentration range of 0.4 to 2 μM. Utilizing the $3\sigma/k$ criterion, where σ represents the standard deviation of ten blank tests and k is the slope of the linear plot, the detection limit (LOD) was assessed to be as low as 150 nM (equivalent to 43.46 ng/mL) (Figure 5c). The detection limit of this method is significantly lower than the reported hepatotoxicity threshold of FKB (LD_{50} = 32 μM), highlighting the exceptional sensitivity of the sensor.[9] The sensor's specificity for distinguishing the target from non-target interferents, including FKA, FKC, myricetin, and quercetin, was rigorously tested (Figure 5d). The results indicated that the aptasensor exhibited negligible response to these interferents compared to the buffer or even lower signals towards the derivatives FKA and FKC, thereby demonstrating its high specificity (Figure 5e). Furthermore, the sensor possesses a favorable detection window. Upon the introduction of the analyte, the absorbance of the test solution promptly increased within 5 minutes and maintained stability for over 10 minutes.